

APPLICATION OF NEURAL NETWORK IN RELIABILITY PREDICTION OF SEISMICLY ISOLATED STRUCTURES SUBJECTED TO RANDOM GROUND MOTIONS

Hesamaldin MOEINDARBARI

PhD Candidate, Amirkabir University of Technology, Tehran, Iran
hessammoen@aut.ac.ir

Touraj TAGHIKHANY

Assistant Professor, Amirkabir University of Technology, Tehran, Iran
ttaghikhany@aut.ac.ir

Keywords: Neural Network, Reliability, Base Isolation, Friction Pendulum

ABSTRACT

One of the most effective technologies of seismic resistant design of structures is base isolation which has lots of different types due to their mechanical behavior. In this study Friction Pendulum Bearings (FPBs) as one of the popular types of base isolation is applied on a specified structure.

Due to stochastic nature of variables such as input ground motion; a novel method is proposed to predict the reliability of the supposed structure using artificial neural networks (ANN). The reliability of the system in the format of probability of failure (Pf) is calculated using a simulation based method which is an effective tool for an isolated structure subjected to random earthquake excitations.

A 2D concrete frame three-story structure isolated with FPB, representing critical facilities, such as a data center, is considered as the super structure. The super structure is designed for gravitational and lateral loads based on ACI 318-05.

Random excitations are applied by the means of artificial earthquake ground motions generated through the superposition of a random ground velocity record with a single, coherent, long-period velocity pulse. The probability of failure for a particular set of structure and isolation parameters was calculated using Monte Carlo Simulation by time history structural analysis at first. Then a set of neural networks were trained to predict the peak responses of the structure. Six random parameters of artificial earthquake ground motion were assumed to be the input variables of neural networks. The probability of failure was calculated again, using neural networks. The results show a good compatibility to the ones calculated using time history structural analysis.

INTRODUCTION

Nowadays, seismic isolation as an advanced effective technology in seismic resistant design of structures has attracted lots of engineers' attentions. Using low stiffness equipment at the base of the building to elongate the period of vibration is the principle role of base isolation that leads to reduction of seismic force response of the structure. Among different types of implemented isolators, Friction Pendulum System (FPS), a first generation of friction concave isolators, is one of the famous systems that was invented by Zayas in 1986 (Zayas, Low et al. 1990). Lots of studies were conducted to this type of isolation systems later (Constantinou, Mokha et al. 1990, Mokha, Constantinou et al. 1990). FPS consists of a spherical concave sliding surface and a slider as an innovative bearing that exerts friction as supplemental damping.

Within the issue of controllable seismic isolation systems, studies are mainly developed through deterministic analyses while the isolation system characteristics, structural system properties, earthquake characteristics, and device properties have inherent uncertainties. Stochastic nature of variables such as input

ground motion encouraged the scientists to apply the probabilistic analyses in structural dynamics, structural reliability methods, and reliability based analysis (Lin and Cai, Ayyub and McCuen 2011). Thus several studies have been conducted on the reliability analysis of isolated structure considering uncertainties in structure, base isolation or ground motion characteristics (Su and Ahmadi 1988, Constantinou and Papageorgiou 1990).

Simulation based methods of reliability analysis is an effective tool to calculate the probability of failure (P_f) or reliability index (β) of an isolated structure subjected to random earthquake excitations (Alhan and Gavin 2005). The big problem in the simulation based reliability methods is the problem of time. For complex systems and for cases where it is difficult to obtain the joint probability distribution function, the probability of failure is evaluated via Monte Carlo Simulations (MCS) by determining the number of realizations with non-positive limit states ($g(X) \leq 0$) and dividing that number by the total number of simulations. Mostly the required number of simulations is too large and for complex dynamic analysis it would take a long time to do the reliability analyses. Regarding this fact several modified MCS methods have been developed to reduce the size of calculations. For this reason a lots of sampling variance reduction techniques have been developed in order to improve the computational efficiency of the method by minimizing the sample size and reducing the statistical error that is inherent in MCS. Hitherto, the introduced sampling techniques can be summarized as; importance sampling, adaptive sampling technique, stratified sampling, Latin hypercube sampling, antithetic variate technique, conditional expectation technique, average sampling and asymptotic sampling (Papadrakakis, Tsompanakis et al. 2004, Iman 2008, Bucher 2009).

Other efficient newly developed methods of simulation based reliability analyses are based on the estimation of the limit states by response surface. These methods are generally called Response Surface Methods (RSM) that are mainly used in Reliability Based Design Optimization (RBDO) (Gosavi 2003). One of the most applicable tools in RSM is Artificial Neural Network (Farooq Anjum, Tasadduq et al. 1997, Papadrakakis and Lagaros 2002, Desai, Survase et al. 2008).

In this study a 2D isolated three story concrete frame purposed for stochastic analyses (Figure 1). The frame is designed for gravitational and lateral loads based on ACI 318-05.

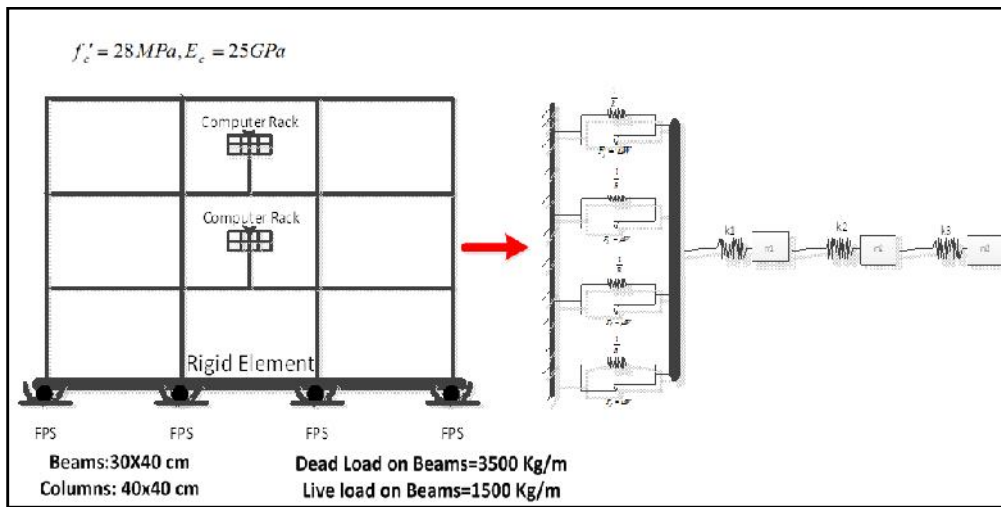


Figure 1. 2D 3-story concrete frame used in simulation and its simplified model

The probability of failure or limit state probability for this system is defined using a limit state function which is defined as the case where the facility floor accelerations reach a 100 milli-g acceleration level. Acceleration levels in the range of 100–200 milli-g are specified by computer producers for sensitive computers as the limit where they fail to operate (Alhan and Gavin 2005). This can be formally stated with the limit state function:

$$g(X) = 100 - |a_i| \quad (1)$$

Where a_i is the peak acceleration of the floor with facility installed, in milli-g. Then the probability of failure is:

$$P_f = P[g(X) \leq 0] \quad (2)$$

The probability of failure for a particular set of structure and isolation parameters was calculated using Monte Carlo Simulation at first. Then a set of neural networks were trained to estimate the peak responses of the structure. Six random parameters of artificial earthquake ground motion were assumed to be the input variables of neural networks. The probability of failure was calculated again, using neural networks. The results show a good compatibility to the ones calculated using time history structural analysis.

MECHANICAL BEHAVIOR OF FPS (SINGLE FP BEARINGS)

Single FP bearings are devices which support vertical load and transmit horizontal loads in a predefined manner through an articulated slider which slides on a concave surface with a radius R and friction coefficient μ as indicated in the figure.

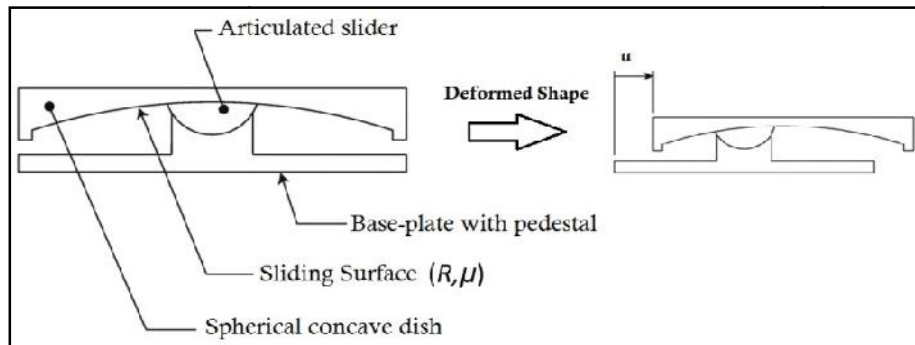


Figure 2. A schematic of single FP bearing

The behavior of the isolation system, described originally by Zayas et al. (Zayas, Low et al. 1990), is based on the pendulum motion: the center of the spherical concave plate follows a circular trajectory so that the motion is that of a pendulum having a length equal to the radius of curvature R .

From the equilibrium of forces acting on the bearing in the vertical and horizontal directions, the force-displacement relationship, that governs the motion of the FP bearing, is:

$$F = \left(\frac{W}{R}\right)u + \sim w \operatorname{sign}(\dot{u}) \quad (3)$$

where u is the horizontal displacement of the pivot point of the slider, sign denotes the signum function of the sliding velocity \dot{u} , R is the radius of curvature of the spherical surface, W is the weight on the bearing and μ is the coefficient of sliding friction, variable with several factors, in particular sliding velocity (Lomiento, Bonessio et al. 2013). Other factors such as load effect, cycling effect and breakaway effect (Lomiento, Bonessio et al. 2013) that changes the friction coefficient in motion, was neglected in this study. The dependency of coefficient of friction to the velocity is given by the following equation (Constantinou, Mokha et al. 1990, Mokha, Constantinou et al. 1990):

$$\sim = f_{\max} - (f_{\max} - f_{\min}) \exp(-a|\dot{u}|) \quad (4)$$

Where f_{\max} is the friction coefficient due to high velocities, f_{\min} is the friction coefficient in lowest (or negligible) velocities and a is the rate parameter that adjusts the rate of the transition of friction coefficient between f_{\max} and f_{\min} .

The resisting force F is sum between the pendulum component, directed towards the center bearing, and the friction component, acting in opposite direction of instantaneous velocity. The fundamental period of vibration of the system, T , related only to pendulum component, is independent of the mass of the structure and related only to the radius of curvature of the spherical surface R .

$$T = 2\pi \sqrt{\frac{R}{g}} \quad (5)$$

INPUT GROUND MOTION

The isolated structure is subjected to random excitation using artificial earthquake ground motions generated through the superposition of a random ground velocity record with a single, coherent, long-period velocity pulse. In this process six random parameters play key role in generation of the artificial acceleration signal. Due to mechanical behavior of FPS, time history analysis can accurately predict the response of an isolated structure with FPS. So the best way to consider the uncertainty of the ground motion is to apply artificially generated signals of earthquakes. Penzien and Watabe (Penzien and Watabe 1974) have shown that the horizontal components of earthquake ground motions that are generated artificially need not be correlated as long as they are directed along a set of principal axes. For single FP bearings, the properties of isolation system in all directions are the same in all directions so a single-directional ground motion and a 2D frame was considered for this study.

Previous studies describe methods for determining the suitable earthquake duration time. Naeim et al. (Naeim, Anderson et al. 1994) organized a database of earthquake records which contains more than 5000 earthquakes with magnitudes greater than 5.5 for the time period 1933–1992 to represent the North American and Hawaiian regions. They provided the bracketed duration corresponding to a 0.05g acceleration level which is defined by Bolt (Bolt 1973) as the duration of an earthquake between the first and last occurrences of accelerations equal to or larger than 0.05g. The 0.05g bracketed duration for the 40 earthquake records provided by Naeim et al. (Naeim, Anderson et al. 1994) lies within 4.4 and 40.8 s. Analysis of nearly 400 time history records from Western USA and Japan by Murphy and O'Brien (Murphy and O'Brien 1977) showed that, on the basis of the duration parameter defined as the interval between the first and last times the acceleration exceeds 25% of the maximum recorded acceleration on a particular component of motion, the range of duration of earthquakes is 2–100 s and most of the values fall in the 25–40 s range. On the basis of these findings, earthquake duration of 30 s is used for the artificially generated earthquake records in our simulations.

The artificial earthquake ground motions used in this study are generated through the superposition of a random ground velocity record with a single, coherent, long-period velocity pulse. The random ground motion velocity record is generated by first simulating an unscaled random ground acceleration record (Alhan and Gavin 2005).

$$a_u(t) = e(t) \sum_{k=1}^{N+1} \left[\frac{1 + (2'_{g_k} f_k / f_g)^2}{(1 - (f_k / f_g)^2)^2 + (2'_{g_k} f_k / f_g)^2} \right]^{1/2} \times \sin(2f_k t + W_k) \quad (6)$$

Where the envelope function $e(t)$ is

$$e(t) = \begin{cases} (t / T_1)^2 & ; 0 \leq t \leq T_1 \\ 1 & ; T_1 \leq t \leq T_2 \\ \exp(-(t - T_2) / T_c) & ; T_2 \leq t \leq T \end{cases} \quad (7)$$

Where $'_g$ and f_g are ground motions damping and frequency parameters and W_k is a random phase angle, uniformly distributed between 0 and 2π . Further, f_k is calculated as:

$$f_k = f_{\min} + (k - 1)(f_{\max} - f_{\min}) / N \quad (8)$$

.An unscaled random ground velocity record $v_u(t)$ is calculated from integral of $a_u(t)$ using the trapezoidal rule and the scaled random ground velocity record is:

$$v_s(t) = v_u(t) (S_v / \max |v_u(t)|) \quad (9)$$

Where S_v is the desired peak of the random ground velocity record. The artificial ground velocity record is then found by combining the scaled random ground velocity with a velocity pulse.



$$v_g(t) = v_s(t) + V_p \exp \left[-2.632 \left(\frac{t - T_1}{N_c T_p} \right)^2 \right] \times \cos \left(2f \frac{t - T_1}{T_p} \right) \quad (10)$$

Where V_p is the peak pulse velocity, N_c is the number of cycles in the pulse, and T_p is the period of the pulse. The artificial ground acceleration record $a_g(t)$ is found by differentiating $v_g(t)$ using central differences. In this study, $T = 30$ s, $f_{min} = 0.5$ Hz, $f_{max} = 20$ Hz, $N = 500$, $T_1 = 6$ s, $T_2 = 9$ s, $T_c = 7.5$ s, and $N_c = 1$.

For random variables $S_v, f_g, 'g, V_p, T_p$, Weibull distribution is considered for random generation of these variables. Then if R represent these 5 variable,

$$R = r[-\log(1-U)]^{1/s} \quad (11)$$

Where r is the scale parameter and s is the shape parameter of the Weibull probability density function, and U is a uniformly distributed random number, between 0.0 and 1.0. The scale parameters of these variables are functions of the distance to the hypocenter, D , and the shape parameters are constants, as shown in Table 1. These shape and scale parameters are selected such that the generated ground motion parameters follow the attenuation relationship reported by Seed and Idriss (Seed and Idriss 1982) for magnitude 6.0 earthquakes in Southern California. In this study, the hypocentral distance, D , is uniformly distributed in the range of 0–100 km (Alhan and Gavin 2005).

Table 1. Scale and shape parameter of Weibull distribution for random variables

Variable	Unit	r	S
S_v	cm / s	$40 / (1 + D^2 / 200)$	3
f_g	Hz	$3 / (1 + D / 50)$	10
$'g$		$0.4 + 0.0005D$	10
V_p	cm / s	$165 / (1 + D_2 / 10)$	3
T_p	s	$3 / (1 + D / 40)$	5

NEURAL NETWORKS

Only the basic ideas of NN will be discussed in this study. A more detailed introduction to NN may be found in (McClelland, Rumelhart et al. 1986). Neural net models of learning and the accumulation of expertise have found their way into practical applications in many areas. It appears that a number of computational structures technology applications, that are heavily dependent on extensive computer resources, have been investigated, showing the range of application of neural network capabilities (Shieh 1994, Adeli and Park 1995, Topping and Bahreininejad 1997, Papadrakakis and Lagaros 2002). Reliability analysis of ultimate elastic plastic structural response using MCS is a highly intensive computational problem which makes conventional approaches incapable of treating real scale problems even in today's powerful computers. In the present study the use of NN was motivated by the approximation concepts inherent in reliability analysis. The idea here is to train a NN to provide computationally inexpensive estimates of the limit state. The major advantage of a trained NN over the conventional numerical process, is that results can be produced in a few clock cycles, requiring orders of magnitude less computational effort than the conventional computational process.

BACK PROPAGATION LEARNING ALGORITHM

The basic model for an artificial neuron is shown in Figure 3. A neural network consists of multiple artificial neurons linked together. In a back propagation (BP) algorithm, learning is carried out when a set of input training patterns is propagated through a network consisting of an input layer, one or more hidden layers and an output layer as shown in Figure 4 in a fully connected NN. Each layer has its corresponding neurons or nodes and weight connections. A single training pattern is an I/O vector of pairs of input output values in the entire matrix of I/O training set.

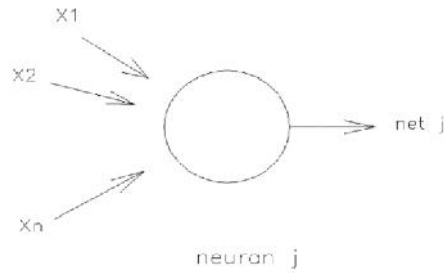


Figure 3. Basic model for an artificial neuron.

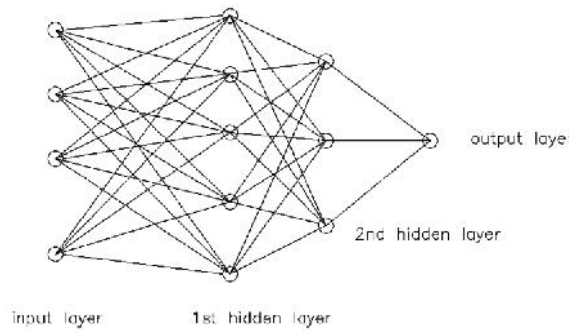


Figure 4. Three layered fully connected NN configuration

The inputs $x_i, i = 1, 2, \dots, n$ which are received by the input layer are analogous to the electrochemical signals received by neurons in human brain. In the simplest model these input signals are multiplied by connection weights $w_{p,ij}$ and the effective input $net_{p,j}$ to neurons is the weighted sum of the inputs:

$$net_{p,j} = \sum_{i=1}^n w_{p,ij} net_{q,i} \tag{12}$$

Where $w_{p,ij}$ is the connecting weight of the layer p from the i neuron in the q (source) layer to the j neuron in the p (target) layer, $net_{q,i}$ is the output produced at the i neuron of the layer q and $net_{p,j}$ is the output produced at the j neuron in the layer p , as shown in Figure 5. Inputs x_i correspond to $net_{q,i}$ for the input layer. In the biological system, a typical neuron may only produce an output signal if the incoming signal builds up to a certain level. This output is expressed in NN by

$$out_{p,j} = F(net_{p,j}) \tag{13}$$

where F is an activation function which produce the output at the j neuron in the p layer. The type of activation function that has been used, for the case of the hidden layers, in the present study is the sigmoid function, while for the case of the output layer the hard limit transfer function is also employed. The sigmoid activation function is given by the expression:

$$F(net_{p,j}) = \frac{1}{1 + e^{-(net_{p,j} + b_{p,j})}} \tag{14}$$

where $b_{p,j}$ is a bias parameter used to modulate the neuron output. The principal advantage of the sigmoid function is its ability to handle both large and small input signals. The determination of the proper weight coefficients and bias parameters is embodied in the network learning process. The weight and bias parameters of the nodes are initialized arbitrarily. The bias parameters are the weights of special connections to each neuron having unity as input value.

At the output layer the computed output(s), otherwise known as the observed output(s), are subtracted from the desired or target output(s) to give the error signal:

$$err_{k,i} = tar_{k,i} - out_{k,i} \tag{15}$$



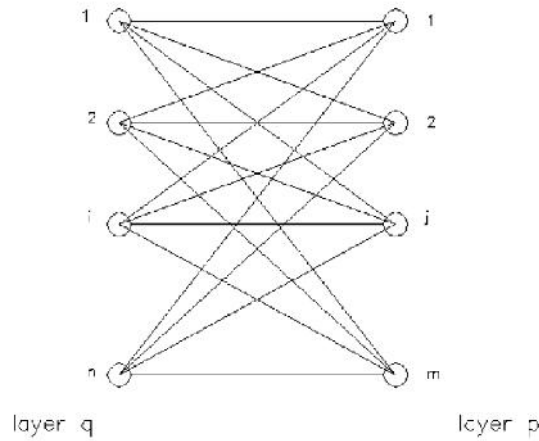


Figure 5. Connection pattern between two layers.

where $tar_{k,i}$ and $out_{k,i}$ are the target and the observed output(s) for the node i in the output layer k , respectively. This is called supervised learning. For the output layer the error signal, as given by Eq. (15), is multiplied by the derivative of the activation function, for the neuron in question, to obtain:

$$u_{k,i} = dF(net_{k,i}) \cdot err_{k,i} \quad (16)$$

while the derivative of the sigmoid function dF is given by:

$$dF(net_{k,i}) = out_{k,i} \cdot (1 - out_{k,i}) \quad (17)$$

Subsequently $u_{k,i}$ is used for the evaluation of the weight changes in the output layer k according to:

$$\Delta w_{k,ji} = \eta \cdot u_{k,i} \cdot out_{p,j} \quad (18)$$

where η denotes a learning rate coefficient usually selected between 0.01 and 0.9 and $out_{p,j}$ is the output of node j of the layer p immediately before the output layer. This learning rate coefficient is analogous to the step size parameter in the numerical optimization algorithms.

The changes in the weights may alternatively be expressed by:

$$\Delta w_{k,ji}^{t+1} = \eta \cdot u_{k,i} \cdot out_{p,j} + \alpha \cdot \Delta w_{k,ji}^t \quad (19)$$

which is adopted in this study, where the superscript t denotes the cycle of the weight modification and α is the momentum term which controls the influence of the previous weight change. For the hidden layers the corresponding weight changes are given by

$$u_{q,j} = dF(net_{q,j}) \sum_{i=1}^n u_{p,i} \cdot w_{p,ji} \quad (20)$$

$$\Delta w_{q,lj}^{t+1} = \eta \cdot u_{q,j} \cdot out_{r,l} + \alpha \cdot \Delta w_{q,lj}^t \quad (21)$$

where $out_{r,l}$ denotes the output of the neuron l in the hidden layer r , $\Delta w_{q,lj}^t$ is the weight, changes between neuron l in the hidden layer r to neuron j in the hidden layer q which is located between the r and p hidden layers.

After the evaluation of the weight changes the updated values of the weights given by $w_{q,ij}^{t+1} = w_{q,ij}^t + \Delta w_{q,ij}^{t+1}$, are used for the next training cycle until the desired level of error is obtained. The procedure used in this study is the single pattern training where all the weights are updated before the next training pattern (training example) is processed.



THE NN TRAINING

In our implementation the main objective is to investigate the ability of the NN to predict the structural maximum responses instead of time history analysis. This objective comprises the following tasks: (i) Select the proper training set. (ii) Find suitable network architecture. (iii) Determine the appropriate values of characteristic parameters, such as the learning rate and momentum term. For the BP algorithm to provide good results the training set must include data over the entire range of the output space. The appropriate selection of I/O training data is one of the important factors in NN training. Although the number of training patterns may not be the only concern, the distribution of samples is of greater importance. The selection of the I/O training pairs is based on the requirement that the full range of possible results should be represented in the training procedure.

The number of neurons to be used in the hidden layers is not known in advance and usually is estimated by trial and error. At the first phase of learning it is convenient to start with an increased number of hidden units and then, after achieving the desired convergence, to try to remove some of them in order to find the minimal size of the network which performs the desired task.

The learning rate coefficient and the momentum term are two user-defined BP parameters that affect the learning procedure of NN. The training is sensitive to the choice of these net parameters. The learning rate coefficient, employed during the adjustment of weights, is used to speed-up or slow-down the learning process. A bigger learning coefficient increases the weight changes, hence large steps are taken towards the global minimum of error level, while smaller learning coefficients increase the number of steps taken to reach the desired error level. If an error curve shows a downward trend but with poor convergence rate the learning rate coefficient is likely to be too high. Although these learning rate coefficients are usually taken to be constant for the whole net, local learning rate coefficients for each individual layer or unit may be applied as well.

The basic NN configuration employed in this study is selected to have one hidden layer. Tests performed for more than one hidden layer showed no significant improvement in the obtained results. The convergence of the training process is controlled by the prediction error. This is done either with a direct comparison of the predicted with the target results computed by the conventional procedure, also called “exact”, or by means of the root mean square (RMS).

After the selection of the suitable NN architecture and the performance of the training procedure, the network is then used to produce predictions of limit state function corresponding to different values of the input random variables. The results are then processed by means of MCS to calculate the probability of failure p_f .

RESULTS

To examine the efficiency of the artificial neural network, nine set of FP bearings with different specifications were considered for simulations (Table 2).

Table 2. Specification of nine set of FP bearings used for simulations

Name	Radius of Curvature (m)	Friction Coefficient
FPB1	1.5	0.1
FPB2	1.5	0.05
FPB3	1.5	0.15
FPB4	3	0.1
FPB5	3	0.05
FPB6	3	0.15
FPB7	4.5	0.1
FPB8	4.5	0.05
FPB9	4.5	0.15

For each set, 500 simulations were done. For these numbers of simulations 500 random artificial earthquakes was generated and used as input ground motion for nonlinear time history analysis of structure. In random generation of artificial earthquake, six random parameters play key role in generation of the artificial acceleration signal: D distance to the hypocenter, S_v the desired peak of random ground velocity, f_g frequency parameter, γ_g ground motion damping, V_p peak pulse velocity and T_p which is the period of pulse; these six parameters used as the input parameters for training the NNs. Absolute values of maximum



story accelerations of the proposed equipped building were used for NN training process as outputs . For each set, 2 individual NN were created to predict the maximum story acceleration of equipped stories (story 1 and story 2).

Therefore the P_f were estimated using the results of 5000 simulations of trained NNs and nonlinear time history structural analysis, for each set of FP bearings. Table 3 and Figure 6 show the results.

Table 3. Probability of failure for different sets of FPB, using NN and Structural analysis for stochastic simulations

Story 1									
P_f	FPB1	FPB2	FPB3	FPB4	FPB5	FPB6	FPB7	FPB8	FPB9
NN (P_{f1})	0.2454	0.2616	0.2310	0.2377	0.2583	0.2350	0.2366	0.2582	0.2346
Structural Analysis (P_{f2})	0.2420	0.2601	0.2300	0.2364	0.2566	0.2364	0.2348	0.2570	0.2312
$e(\%) = \frac{ P_{f1} - P_{f2} }{P_{f2}} \times 100$	1.40	0.58	0.43	0.55	0.66	0.59	0.77	0.47	1.47
Story 2									
P_f	FPB1	FPB2	FPB3	FPB4	FPB5	FPB6	FPB7	FPB8	FPB9
NN (P_{f1})	0.3506	0.3148	0.3635	0.3565	0.3174	0.3657	0.3496	0.3175	0.3668
Structural Analysis (P_{f2})	0.3526	0.3153	0.3620	0.3547	0.3155	0.3643	0.3511	0.3159	0.3634
$e(\%) = \frac{ P_{f1} - P_{f2} }{P_{f2}} \times 100$	0.57	0.16	0.41	0.51	0.60	0.38	0.43	0.51	0.94

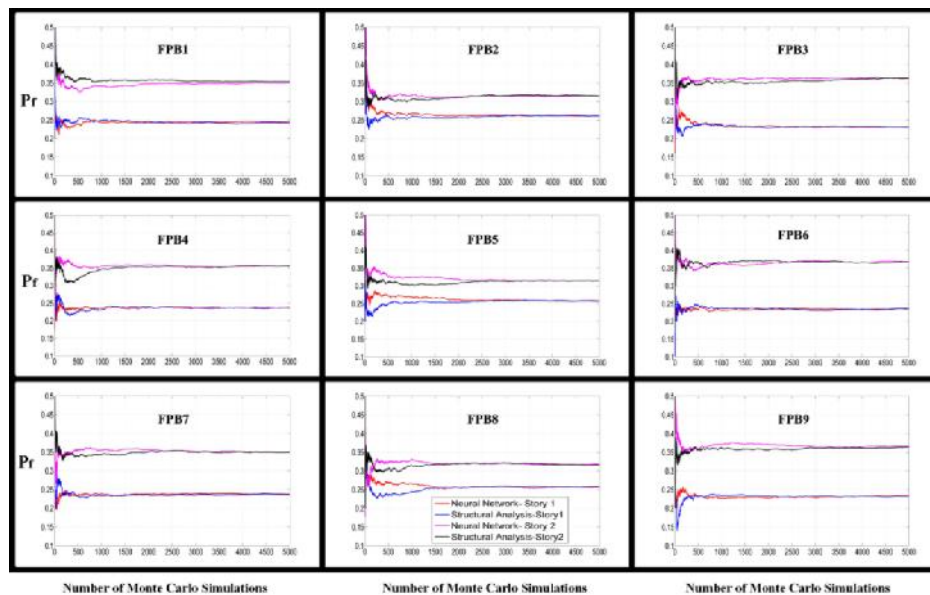


Figure 6. Convergence of P_f using NN and Structural analysis for 9 sets of FPBs

CONCLUSIONS

According to the results, probability of failure obtained by NN shows good compatibility with the ones obtained by structural time history analysis. Considering reduction in the numbers of structural time history analysis, the errors listed in Table 3, are negligible. In the proposed method the number of time history analysis can be decreased to one-tenth. This amount of reduction can significantly reduce the calculation time. This advantage can significantly improve the efficiency of optimization algorithms in reliability based design of isolated structures.

REFERENCES

- 6(2): 317-333 Adeli Hand Park HS (1995) Optimization of space structures by neural dynamics." *Neural Networks* 8(5): 769-781
- Alhan C and Gavin HP (2005) Reliability of base isolation for the protection of critical equipment from earthquake hazards. *Engineering Structures* 27(9): 1435-1449

- Ayyub BM and McCuen RH (2011) Probability, statistics, and reliability for engineers and scientists, CRC press
- Bolt BA (1973) Duration of strong ground motion. *Proceedings of the 5th world conference on earthquake engineering*
- Bucher C (2009) Computational Analysis of Randomness in Structural Mechanics: Structures and Infrastructures Book Series, CRC Press
- Constantinou MA, Mokha and Reinhorn A (1990) Teflon bearings in base isolation II: Modeling. *Journal of Structural Engineering* 116(2): 455-474
- Constantinou Mand Papageorgiou A (1990) Stochastic response of practical sliding isolation systems. *Probabilistic Engineering Mechanics* 5(1): 27-34
- Desai KM, Survase SA, Saudagar PS, Lele S and Singhal RS (2008) Comparison of artificial neural network (ANN) and response surface methodology (RSM) in fermentation media optimization: case study of fermentative production of scleroglucan. *Biochemical Engineering Journal* 41(3): 266-273
- Farooq Anjum, Tasadduq MI and Al-Sultan K (1997) Response surface methodology: A neural network approach. *European Journal of Operational Research* 101(1): 65-73
- Gosavi A (2003) Simulation-based optimization: parametric optimization techniques and reinforcement learning, Springer
- Iman RL (2008) Latin hypercube sampling, Wiley Online Library
- Lin Y and Cai G (1995) Probabilistic structural dynamics: advanced theory and applications. 1995, McGraw-Hill, New York
- Lomiento G, Bonessio N and Benzoni G (2013). "Friction Model for Sliding Bearings under Seismic Excitation." Journal of Earthquake Engineering 17(8): 1162-1191.
- McClelland JL, Rumelhart DE and Group PR (1986) Parallel distributed processing. Explorations in the microstructure of cognition 2
- Mokha A, Constantinou M and Reinhorn A (1990) Teflon bearings in base isolation I: Testing. *Journal of Structural Engineering* 116(2): 438-454
- Murphy J and O'Brien (1977) The correlation of peak ground acceleration amplitude with seismic intensity and other physical parameters. Bulletin of the Seismological Society of America 67(3): 877-915
- Naeim F, Anderson J and Jain S (1994) A database of earthquake records for design. Proceedings of the 5th US National Conference on Earthquake Engineering.
- Papadrakakis M and Lagaros ND (2002) "Reliability-based structural optimization using neural networks and Monte Carlo simulation." Computer Methods in Applied Mechanics and Engineering 191(32): 3491-3507.
- Papadrakakis M, Tsompanakis Y, Lagaros ND and Fragiadakis M (2004) Reliability based optimization of steel frames under seismic loading conditions using evolutionary computation. *Journal of Theoretical and Applied Mechanics* 42(3): 585-608
- Penzien J and Watabe M (1974) Characteristics of 3-dimensional earthquake ground motions. *Earthquake Engineering & Structural Dynamics* 3(4): 365-373
- Seed HB and Idriss I (1982) Ground motions and soil liquefaction during earthquakes, Earthquake Engineering Research Institute Berkeley, CA
- Shieh RC (1994) Massively parallel structural design using stochastic optimization and mixed neuralnet/finite element analysis methods. *Computing Systems in Engineering* 5(4): 455-467
- Su L and Ahmadi G (1988) Response of frictional base isolation systems to horizontal-vertical random earthquake excitations. *Probabilistic Engineering Mechanics* 3(1): 12-21
- Topping BH and Bahreininejad A (1997) Neural computing for structural mechanics, Saxe-Coburg Publications
- Zayas VA, Low SS and Mahin SA (1990) A simple pendulum technique for achieving seismic isolation. *Earthquake Spectra*



